simulations based on the MoM, Ensemble v.5.1, and measurements. Finally, this model has been applied to the synthesis of two antennas presented in [19, 20] and very accurate results have been obtained.

REFERENCES

1. M. Sierra Pérez, M. Vera Isasa, A. García Pino, and M. Sierra Castañer, Analysis of slot antennas on a radial transmission line, Int J Microwave Millimeter Wave CAE 6 (1996), 115–127.
2. F.J. Goebels, Jr. and K.C. Kelly, Arbitrary polarization from annular slot planar antennas, IRE Trans Antennas Propagat AP-9 (1961), 342–349.
3. M. Ando, K. Sakurai, N. Goto, K. Arimura, and Y. Ito, A radial line slot antenna for 12-GHz satellite TV reception, IEEE Trans Antennas Propagat AP-33 (1985), 1347–1353.
4. M. Ando, K. Sakurai, and N. Goto, Characteristics of a radial line slot antenna for 12-GHz band satellite TV reception, IEEE Trans Antennas Propagat AP-34 (1986), 1269–1272.
5. H. Sasazawa, Y. Oshima, K. Samurai, M. Ando, and N. Goto, Slot coupling in a radial line slot antenna for 12-GHz band satellite TV reception, IEEE Trans Antennas Propagat AP-36 (1988), 1221–1226.
6. E. Rammos, New wideband high-gain stripline planar array for 12 GHz satellite TV, IEE Electron Lett 18 (1982), 252–253.
7. J.C. Williams, A 36-GHz printed planar array, IEE Electron Lett 14 (1978), 136–137.
8. M. Takahashi, J. Takada, M. Ando, and N. Goto, A slot design for uniform aperture field distribution in single-layered radial line slot antennas, IEEE Trans Antennas Propagat 39 (1991), 954–959.
9. K. Kechagias, E. Vafiadis, and J. Sahalos, On the RLSA antenna optimum design for DBS reception, IEEE Trans Broadcasting 44 (1998), 460–469.
10. M. Vera, Diseño de Antenas de Ranuras sobre Guía Radial, Doctoral disertation, Universidad de Vigo, 1996.
11. A. Akiyama, T. Yamamoto, M. Ando, and N. Goto, Numerical optimisation of slot parameters for a concentric array radial line slot antenna, IEE Proc Microwave Antennas Propagat 145 (1998), 141–145.
12. M. Takahashi, M. Ando, N. Goto, Y. Numano, M. Suzuki, Y. Okazaki, and T. Yoshimoto, Dual circularly polarized radial line slot antenna, IEEE Trans Antennas Propagat 43 (1995), 874–876.
13. J. Takada, A. Tanisho, K. Ito, and M. Ando, Circularly polarised conical beam radial line slot antenna, IEE Electron Lett 30 (1994), 1729–1730.
14. A. Akiyama, T. Yamamoto, M. Ando, and E. Takeda, Conical beam radial line slot antennas for 60 GHz band wireless LAN, IEEE Antennas Propagat Soc Int Symp 3 (1998), 1421–1424.
15. M. Ando, T. Numata, J. Takada, and N. Goto, A linearly polarized radial line slot antenna, IEEE Trans Antennas Propagat 36 (1988), 1675–1680.
16. J. Takada, M. Ando, and N. Goto, A linearly polarized radial line slot antenna reflection cancelling slot set in a linearly polarized radial line slot antenna, IEEE Trans Antennas Propagat 40 (1992), 433–438.
17. P. Davis and M. Bialkowski, Experimental investigations into a linearly polarized radial slot antenna for DBS TV in Australia, IEEE Trans Antennas Propagat 45 (1997), 1123–1129.
18. P. Davis and M. Bialkowski, Linearly polarized radial-line slot-array antennas with improved return-loss performance, IEEE Antennas Propagat Mag 41 (1999), 52–61.
19. M. Sierra-Castañer, M. Sierra-Pérez, M. Vera-Isasa, and J.L. Fernández-Jambrina, Low-cost monopulse radial line slot antenna, IEEE Trans Antennas Propagat 51 (2003), 256–263.
20. M. Sierra-Castañer, M. Sierra-Pérez, M. Vera-Isasa, and J.L. Fernández-Jambrina, Multiprobe RLSA design for DBS reception, Microwave Opt Technol Lett 36 (2003), 70–72.
21. J. Hirokawa, M. Ando, and N. Goto, Analysis of slot coupling in a radial line slot antenna for DBS reception, IEE Proc 137 (1990), 249–254.

RADIATION PROPERTIES OF PIFA ON ELECTROMAGNETIC BANDGAP SUBSTRATES

Y. Zhao, Y. Hao, and C. G. Parini
Department of Electronic Engineering
Queen Mary, University of London
Mile End Road, London E1 4NS, UK

Received 12 June 2004

ABSTRACT: *One of longstanding problems in planar inverted-F antenna (PIFA) design is its radiation pattern, which degrades when the PIFA is placed too close to the conductive ground. It is demonstrated that the use of electromagnetic bandgap (EBG) structures will reduce PIFA backward radiation and hence improve its efficiency. The theoretical prediction is verified through measurements with good agreement.*
 Microwave Opt Technol Lett 44: 21–24, 2005; Published online in Wiley InterScience (www.interscience.wiley.com). DOI 10.1002/mop.20535

Key words: *PIFA; mobile communication; antenna; size reduction*

1. INTRODUCTION

One of the current constraints on antenna design for small handheld devices such as mobile phones, personal digital assistants (PDAs), and wireless wearable computers is the limitation of design space, particularly for some internal antennas such as printed dipoles, meander-line, antennas and planar inverted-F antennas (PIFAs), and so forth. Among them, PIFAs have the features of compactness, moderate bandwidth, high gain for both states of polarization, and reduced special absorption rate (SAR). One of the concerns in mobile handset design is its antenna-size reduction. At present, there are several methods available for reducing PIFA size: the uses of shorting pins [1] and capacitance-loading [2] are common practices. In theory, antenna-size reduction can be achieved when the substrate thickness is reduced. Unfortunately, if the antenna is placed too close to the conductive ground, the phase of the impinging field is reversed upon reflection, resulting in destructive interference and hence poor radiation [3]. Another concern is increased RF power losses in the user's body (mainly in the head), which are radiated from edges of the limited ground plane. electromagnetic bandgap (EBG), also referred as photonic bandgap (PBG) structures [4], offer the opportunity to control and manipulate electromagnetic-wave propagation as a result of their being formed from small-scale periodic geometric structures. Its applications include the suppression of surface waves [5], the construction of perfect magnetic conducting (PMC) planes [6], and the use of anisotropic characteristics of EBGs for designing microstrip diplexer antennas [7]. However, only a few applications can be found on the PIFA design for mobile communications. The application of EBG substrate in PIFA design was investigated by Du et al. using the finite-difference time-domain (FDTD) simulation [8]; however, no experimental results were presented. In this paper, radiation properties of PIFA on a mushroomlike EBG substrate are examined. Specifically, radiation-performance degradation from a conventional PIFA with reduced air gap between the antenna and the ground plane is investigated and compared with that over EBGs. It is demonstrated that the use of EBGs will reduce antenna backward radiation and hence improve its efficiency. Thus, a reduced SAR is also obtainable. The theoretical prediction is verified through measurements with good agreement. All the proposed antennas operate at 2.4 GHz, a standard frequency band for Bluetooth applications.

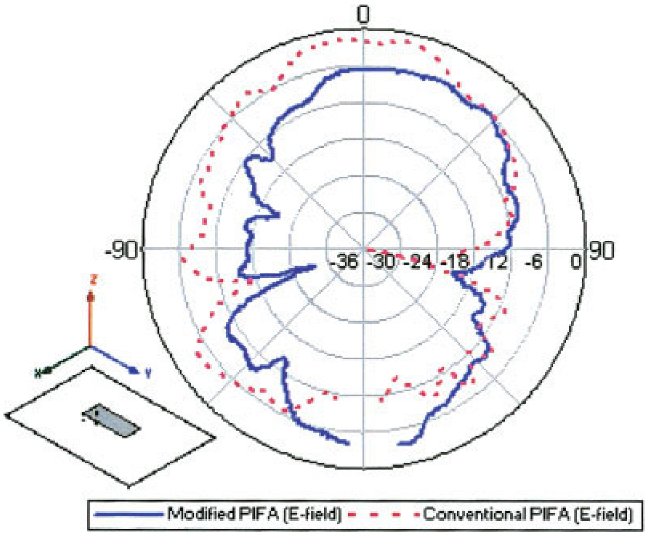

Figure 1 Comparison between the radiation patterns of a conventional PIFA and a modified PIFA. [Color figure can be viewed in the online issue, which is available at www.interscience.wiley.com.]

4. RADIATION DEGRADATION FROM PIFA WITH REDUCED AIR GAP

The resonant frequency f_r of the PIFA over its size can be approximated by [9]:

$$f_r = \frac{c}{4\alpha(l + w)}, \tag{1}$$

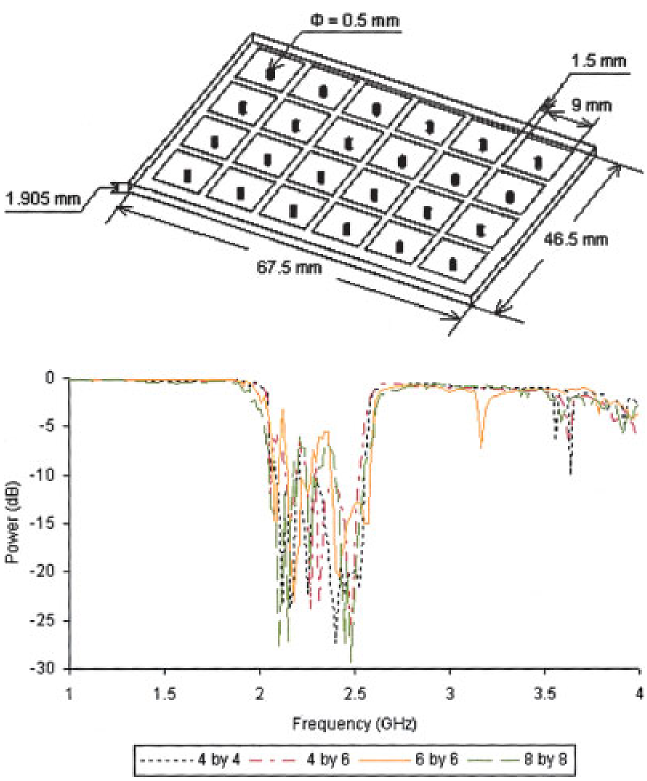

Figure 2 (a) Mushroomlike EBG structure used in HFSS simulation; (b) transmission coefficients (S_{21}) of the proposed EBG structure for different number of elements (square patches): 4×4, 4×6, 6×6, and 8×8. [Color figure can be viewed in the online issue, which is available at www.interscience.wiley.com.]

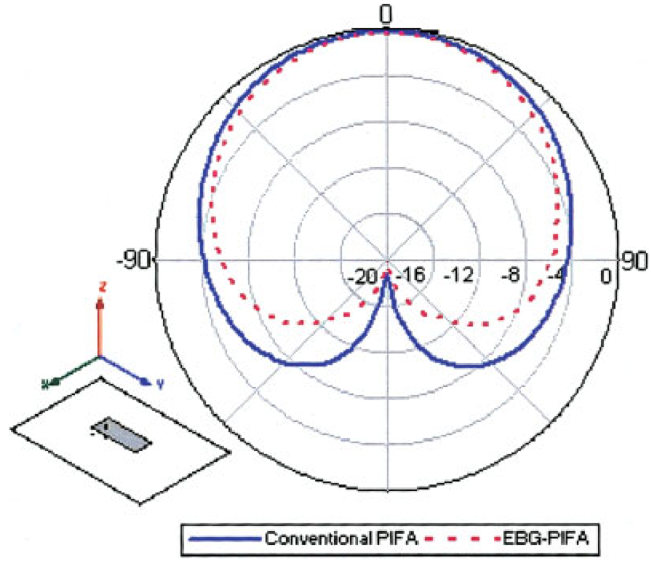

Figure 3 Comparison between the simulated radiation patterns of a conventional PIFA and an EBG-PIFA. [Color figure can be viewed in the online issue, which is available at www.interscience.wiley.com.]

where c is the speed of light, l and w are the length and width of the PIFA element, respectively, and α is a constant of about 0.9.

It is noted that the PIFA radiation and impedance bandwidth are dependent on the separation distance between the radiator and the ground. Generally, the higher the air gap (separation between the PIFA and the ground) is, the greater the obtainable bandwidth and gain can be achieved. However, there is an increasing need for further reducing the PIFA size, in particular, the air-gap distance, in order to make the mobile phone thinner. Figure 3 shows the differences of radiation pattern between the conventional PIFA and the PIFA with a reduced air gap. The conventional PIFA shows considerable backward radiation due to the small ground plane. Such unwanted backward radiation becomes even stronger when the antenna is brought closer to the ground plane, since as more surface waves are excited and radiate from the edges and corners.

3. EBG-PIFA ANTENNA DESIGN

It can be seen from Figure 1 that conventional PIFAs have the limitations of a restricted band operation and a reduction in the radiation efficiency due to the losses caused by backward radiation. Furthermore, PIFA size reduction can lead to decreases in bandwidth and gain. In this section, we will demonstrate that PIFA performance degradation can be mitigated by applying an EBG substrate in order to replace the conventional conductive ground.

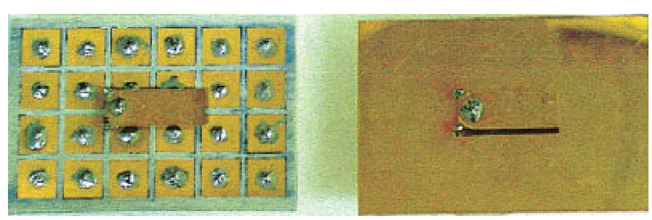

Figure 4 Photographs of an EBG-PIFA and a conventional PIFA. [Color figure can be viewed in the online issue, which is available at www.interscience.wiley.com.]

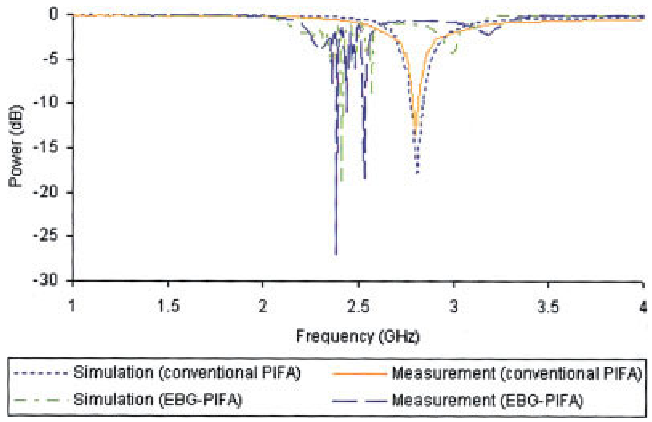

Figure 5 Simulated and measured return losses (S_{11}) of a conventional PIFA and an EBG-PIFA. [Color figure can be viewed in the online issue, which is available at www.interscience.wiley.com.]

EBG structures are capable of controlling the flow of electromagnetic waves. Within the EBG structure, there is a range of frequencies where propagating modes can be fully or partially suppressed in one or more dimensions. This range of frequencies is known as the electromagnetic stopband, or bandgap [10]. Due to these properties, EBGs can provide significant advantages for suppressing and directing radiation, and thus improving efficiency when used in antennas. Compared to other EBG structures, the mushroomlike EBG structure has the highly desired feature of compactness, which is important in communications applications. Its bandgap features are revealed in two ways: (i) the suppression of surface-wave propagation and (ii) the in-phase reflection coefficient. The feature of surface-wave suppression helps to improve antenna performance, for example, by increasing antenna gain and reducing backward radiation [11]; while the in-phase reflection feature leads to low-profile antenna design [12].

Generally, for a planar EBG structure, the centre frequency f_0 of the stopband is determined from $f_0 = c/2S$, where c is the speed of light in free space, and S is the period of structure. For the mushroomlike EBG structure, it consists of four parts: metallic patches, connecting pins, a dielectric substrate, and a ground plane. This structure introduces an inductor L, which results from the current flowing through the vias, and a capacitor C, which is due to the gap effect between adjacent patches. For the structure [Fig. 2(a)] with patch width W, gap width g, substrate thickness h, and dielectric constant ε_r, the values of inductor L and capacitor C can be approximated by the following formulas [3],

$$L = \mu_0 h, \tag{2}$$

$$C = \frac{W\varepsilon_0(1 + \varepsilon_r)}{\pi} \cosh^{-1}\left(\frac{2W + g}{g}\right), \tag{3}$$

where μ_0 is the permeability of free space and ε_0 is the permittivity of free space. Thus, the bandgap can be determined by

$$\omega = \frac{1}{\sqrt{LC}}, \tag{4}$$

$$BW = \frac{\Delta\omega}{\omega} = \frac{1}{\eta}\sqrt{\frac{L}{C}}, \tag{5}$$

where η is the free-space impedance ($\eta = 120\pi$).

However, the formulas only give an approximation of the resonant frequencies, since the effects from metallic vias in the EBG design are not considered. An accurate but complex model using the theory of transmission lines and periodic circuits can be found in [13].

The proposed EBG structure is simulated using the Ansoft HFSS™ 9.0 software. The dimensions are chosen as shown in Figure 2(a): square patches: 9×9 mm^2, patch gaps: 1.5 mm, ground plane: 46.5×67.5 mm^2, dielectric constant (EBG substrate): 9.8, and thickness: 1.905 mm. In theory, a broader bandgap results in a better control of the backward radiation of the antenna; thus, it is essential to put more elements onto the limited mobile-phone ground plane. In total, there are 24 (4×6) elements in the proposed structure, which gives a frequency bandgap from 2.1 to 2.6 GHz [Fig. 2(b)]. Other structures with different numbers of

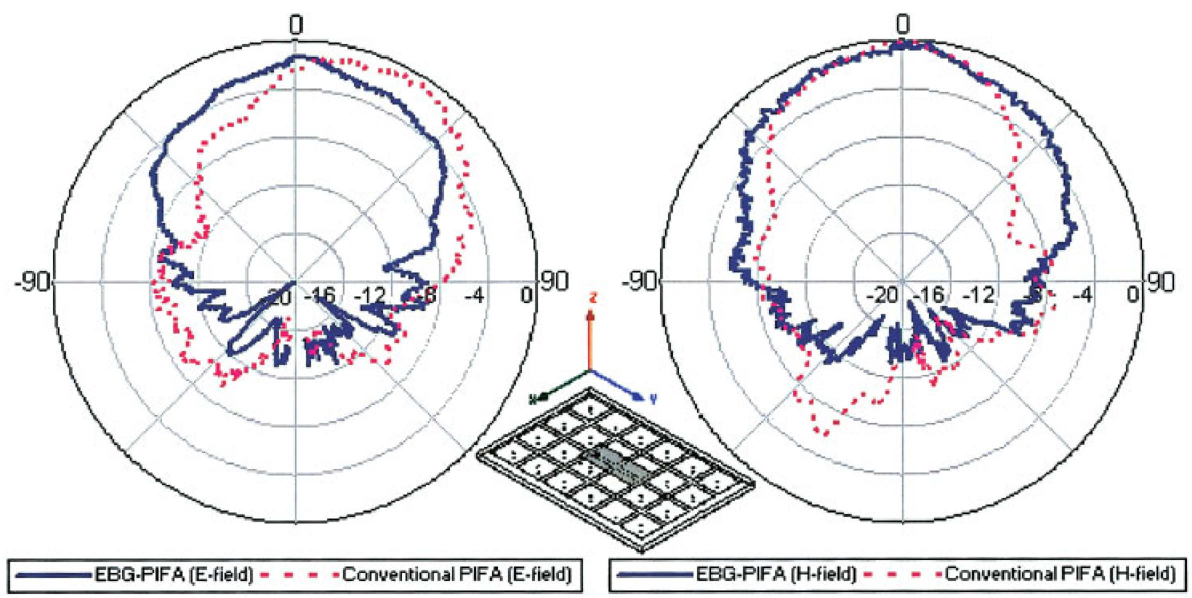

Figure 6 Comparison between the measured radiation patterns of a conventional PIFA and an EBG-PIFA. [Color figure can be viewed in the online issue, which is available at www.interscience.wiley.com.]

elements (4×4, 6×6, and 8×8) have also been simulated, as shown in Figure 2(b). It can be seen that the bandgap region does not shift significantly as the period of structure remains unchanged.

The radiator size of both conventional PIFAs and EBG-PIFAs is 8.4×22.8 mm^2, which is made from a 1-mm-thick copper film with a conductivity of 58.13×10^6 S/m. Two shorting pins are used instead of a shorting strip at one edge of the radiator due to the ease of fabrication. The shorting pins connect the radiator and ground plane through the gap of EBG patches without touching them. The feed point of the EBG-PIFA remains the same as that of the conventional PIFA (3 mm from the shorting edge of the radiator, as shown in Figure 4, while the air gap thickness is set to 3 mm. The ground plane size in the two cases is set to be the same (46.5×67.5 mm^2) as that in the most popular commercial handsets. It can be seen from both the simulation and measurement results (as shown in Fig. 5), that the resonant frequency shifts due to the reduced air gap; hence, this confirms such a potential approach for reducing the PIFA size. The frequency shifts from 2.7 to 2.4 GHz in the HFSS simulation, while it shifts from 2.8 to 2.38 GHz in the measurement. Figure 6 shows the differences of radiation pattern between the conventional PIFA and the PIFA with EBG structure. It is demonstrated that the conventional PIFA with small air gap has strong backward radiation, whereas the EBG-PIFA shows a 6-dB reduction; both the measurement and simulation results show very good agreement. The distance from the radiator patch to the ground plane in the EBG-PIFA is 4.9 mm, (including a 3-mm air gap and a 1.905-mm substrate), compared to the 7.5-mm air gap in the conventional PIFA structure. This leads to a decrease in the mobile-phone thickness by 2.6 mm.

5. CONCLUSION

The radiation properties of planar inverted-F antennas (PIFAs) on electromagnetic bandgap (EBG) substrate have been presented. It was verified experimentally that the EBG structure (even with only 4×6 elements) reduces surface waves, thus leading to an increase in directivity, bandwidth, forward and backward radiation ratios, and efficiency.

REFERENCES

1. P.K. Panayi, M.O. Al-Nuaimi, and I.P. Ivrissimtzis, Tuning techniques for planar inverted-F antenna, Electron Lett 37 (2001), 1003–1004.
2. C.R. Rowell and R.D. Murch, A capacitively loaded PIFA for compact mobile telephone handsets, IEEE Trans Antennas Propagat 45 (1997), 837–842.
3. D.F. Sievenpiper, High-impedance electromagnetic surfaces, Ph.D. thesis, UCLA, 1999.
4. E. Yahlonovitch, Inhibited spontaneous emission in solid state physics and electronics, Phys Rev Lett 50 (1987), 2059–2062.
5. R. Gonzalo, P. De Maagt, and M. Sorolla, Enhanced patch-antenna performance by suppressing surface waves using photonic-bandgap substrates, IEEE Trans Microwave Theory Tech 47 (1999), 2131–2138.
6. Y. Hao and C.G. Parini, Microstrip antennas on various UC-PBG substrates, IEICE Trans Electron E86-C (2003), 1536–1541.
7. Y. Hao and C.G. Parini, Isolation enhancement of anisotropic UC-PBG microstrip diplexer patch antenna, Antennas Wireless Propagat Lett 1 (2002), 135–137.
8. Z.W. Du, K. Gong, J.S. Fu, B.X. Gao, and Z.H. Feng, A compact planar inverted-F antenna with a PBG-type ground plane for mobile communications, IEEE Trans Vehic Technol 52 (2003), 483–489.

THICK-SLOT TRANSITION AND ANTENNA ARRAYS IN THE Q BAND

O. Lafond,[1] M. Himdi,[1] O. Vendier,[2] and Y. Cailloce[2]
[1] Institut d'Electronique et Télécommunications de Rennes (IETR)
UMR CNRS 6164
Université de Rennes I
35042 Rennes Cedex, France
[2] Alcatel Space
26, avenue J.F. Champollion
B.P. 1198
31037 Toulouse Cedex 1, France

Received 12 June 2004

ABSTRACT: *This paper deals with an H-shaped slot etched in a thick ground plane to feed multilayer antenna arrays. This study takes place under the European MIPA project [1], which concerns an antenna prototype that is part of a Q-band (50-GHz) one-feed-per-beam antenna reflector. In millimetre waves, it is highly required to separate active layers (MEMS, MMIC, and so on) and radiating elements in order to avoid electrical spuriousness generated by coupling radiation. This separation is done with a very thick metallic support (2 mm). Moreover, this thick ground plane is important with regard to the thermal dissipation aspect. With this aim, the authors present an original feed of antenna array via an H-shaped thick-slot transition.* © 2004 Wiley Periodicals, Inc. Microwave Opt Technol Lett 44: 24–29, 2005; Published online in Wiley InterScience (www.interscience.wiley.com). DOI 10.1002/mop.20536

Key words: *antenna feed; H-shape slot; technology; millimetre waves*

1. INTRODUCTION

This study takes place under the European project MIPA [1] (MEMS-based integrated phased array antennas), which is focused

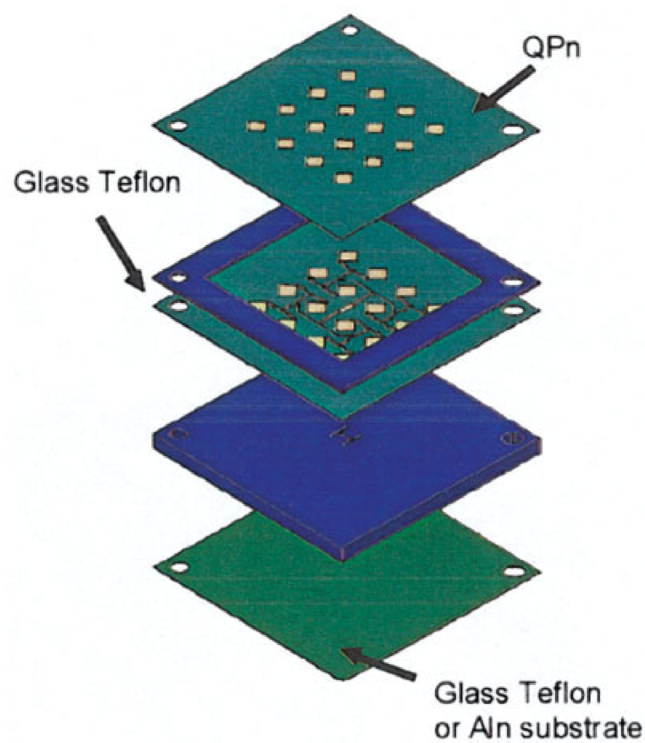

Figure 1 Proposed antenna prototype for spacial communication in the Q band. [Color figure can be viewed in the online issue, which is available at www.interscience.wiley.com.]